

Synchronized clusters and multistability in arrays of oscillators with different natural frequencies

G. V. Osipov*

*The University of Nizhny Novgorod, 23 Gagarin Avenue, 603600 Nizhny Novgorod, Russia
and Center for BioDynamics and Department of Biomedical Engineering, Boston University, 44 Cummington Street,
Boston, Massachusetts 02215*

M. M. Sushchik[†]

*Institute of Applied Physics, Russian Academy of Science, 46 Uljanov Street, 603600 Nizhny Novgorod, Russia
(Received 27 March 1998)*

The collective effects in arrays of diffusively coupled Van der Pol oscillators with different natural frequencies are investigated by asymptotic and numerical methods. The conditions for the onset and existence of the regimes of global (all-to-all) and cluster (inside several subsets of elements) frequency synchronization are determined. It is found that there exist monostable and multistable regimes of cluster synchronization and the respective “soft” and “hard” transitions between the structures consisting of a different number of clusters. It is revealed that the synchronization is observed in a broader range of parameters in a randomly formed array than for regularly arranged oscillators with the natural frequencies varying monotonically along the array. [S1063-651X(98)02012-1]

PACS number(s): 05.45.+b

I. INTRODUCTION

The relationship between the properties of temporal dynamics of oscillations and their changes in space in extended systems and their array analogs has recently been attracting attention of the researchers in terms of both diagnostics [1,2] and feasibility of different regimes [3–5]. The fact that may seem surprising at first sight was established: Under certain conditions time-periodic behavior is realized only in the presence of spatial disorder generated either by the system itself [3] or introduced from the outside, for example, by the dispersion of parameters of the elements in the array [4,5]. In particular, a chaotic regime may be realized in an array of identical non-linear pendulums with external forcing under certain conditions. But this regime is replaced by a periodic one [4] if there is a dispersion in parameters. A similar effect is observed in an analogous mathematical system, but without external periodic forcing, that models a parallel array of current-biased Josephson junctions coupled via inductors. A small dispersion in the currents gives rise to enhanced mutual synchronization of oscillations in these junctions [5]. In the present paper we also analyze the effect of disorder on synchronization but in a slightly different formulation. Specifically: How does the change in the distribution of parameters (natural frequencies in the case of interest) along the array influence synchronization, if the range of their values remains unchanged? We take as an example coupled oscillators in which the dependence of natural frequencies along the array,

$$(j = 1, \dots, N) \quad (1)$$

changes from monotonic, completely regular (for $\Delta\omega^* = 0$) to a completely irregular one (for $\Delta\omega^* = \Delta\omega$). Here, ξ_j are uniformly distributed random numbers in the interval $[-0.5; +0.5]$, N is the number of elements in the array, and $\Delta\omega$ is the interval of frequency dispersion. We choose a regular distribution in the form of linear frequency variation along the array because this case may be of independent interest.

The paper is organized as follows. Arrays of oscillators with uniform frequency mismatch $\Delta\omega_j = \omega_j - \omega_{j-1} = \text{const}$ are investigated in detail in the frame of a discrete analog of Ginzburg-Landau equations in Sec. II. We begin with a brief description of the model (Sec. II A) and characteristics of global synchronization (Sec. II B) that are further used for interpretation of the properties of cluster synchronization (Sec. II C). Multistable regimes are described in Sec. II D. In Sec. III formation of the clusters separated by a region of unexcited oscillators is interpreted in terms of the effect of oscillator death [6–9]. The formation of synchronized clusters in the presence of the regular nonuniformities of frequency mismatch the spatial scale of which is close to the size of the clusters is considered in Sec. IV A. In Sec. IV B it is shown that small-scale nonuniformities, irregular ones inclusive, may expand the region of the parameters in which synchronization is possible. Nonlinear effects that are beyond the scope of Ginzburg-Landau equations are considered in Sec. V on an example of Van der Pol oscillators.

II. SYNCHRONIZATION CLUSTERS AND MULTISTABILITY AT LINEAR VARIATION OF NATURAL FREQUENCIES ALONG THE ARRAY

Arrays of oscillators with the natural frequencies varying linearly along them are interesting both conceptually and because they are encountered in a natural fashion in various

$$\omega_j = \omega_0 + \frac{\Delta\omega^*}{2} + \frac{(j-1)(\Delta\omega - \Delta\omega^*)}{N-1} + \Delta\omega^* \xi_j$$

*Electronic address: osipov@bu.edu

[†]Electronic address: sushch@euler.appl.sci-nnov.ru

situations. We will mention here two rather illustrative examples. One of them concerns dynamics of a mammalian small intestine. If one isolates in them sections 1–3 cm long, then each of them is able to oscillate at a definite frequency, the changes of which along the intestine may be regarded to be linear at rather long distances [10]. The other example, in which linear variations of the local natural frequency along the spatial coordinate are manifested, is the vortex shedding in a flow past cone-shaped bodies (for example, supports or chimney stacks). Such research also involves analysis of an array of coupled oscillators with linearly varying natural frequencies, if the derivative with respect to the coordinate along the cone axis is replaced by finite differences (see, e.g., [11]). In these and other analogous cases, a sufficiently strong coupling between oscillators gives rise to local frequencies of excited collective oscillations that strongly differ from the natural frequencies. Besides, steps in the form of well pronounced and rather extended plateaus that are intermittent with a relatively narrow transition region appear in their dependence on spatial coordinate. We briefly characterize this effect as cluster synchronization. Under a cluster we understand a coupled set of oscillators having the same average period T and the corresponding mean frequency $\Omega \sim T^{-1}$, with no demand for constant phase difference between the elements and with allowance for limited variations in time.

As the control parameter R (frequency gradient along the array, value of coupling, etc.) is changed, the cluster structure is destroyed at $R = R_{\text{cr}}$. On passing the critical value, it is regenerated again at $R = R_{\text{cr}} + \Delta R$ but now with a different number of clusters. A chaotic behavior may appear at $R \in (R_{\text{cr}}, R_{\text{cr}} + \Delta R)$ and, since the relative share of intervals ΔR increases with the increase of the frequency gradient and/or the weakening of coupling, the clusters will eventually disappear in the sea of chaos. A well pronounced scenario of the transition to turbulence through cluster fractioning is still another factor stimulating an interest in the problem considered.

Theoretical investigations of cluster synchronization in arrays with linear frequency variations have been carried out for a long time, including modeling the specific behavior of a mammalian small intestine [10,12–15]. The problem was formulated and analyzed in the general context in [16] in the frame of the phase equation. However, the effects in which amplitude variations are significant were revealed almost simultaneously [17] (see also [18]). A vivid manifestation of these effects is formation of clusters of oscillators with infinitesimal amplitude, even if the conditions of self-excitation in the absence of coupling are fulfilled for each of them. This effect is known as ‘‘oscillator death’’ or ‘‘amplitude death’’ [6–9,19,20]. The amplitude effects are also essential for the formation and restructuring of cluster structures. Therefore here we employ equations for slow complex amplitudes. Their solution is more complicated than analysis of phase equations. Consequently, we have to use partial solutions obtained numerically.

A. Model

The model considered is a one-dimensional array of oscillators (Van der Pol oscillators for definiteness) having dif-

ferent natural frequencies. Each oscillator is coupled diffusively with its two nearest neighbors. The model equations may be written in the form

$$\begin{aligned} \ddot{u} + (\hat{I} + \epsilon \hat{\Delta})^2 u - 2\epsilon(p\hat{I} - \hat{U}^2)\dot{u} &= 2\epsilon d\hat{A} \dot{u}, \\ U_{ij} &= \begin{cases} u_j, & i=j \\ 0, & i \neq j \end{cases} \\ I_{ij} &= \begin{cases} 1, & i=j \\ 0, & i \neq j. \end{cases} \end{aligned} \quad (2)$$

Here, the column vector u and the diagonal matrix \hat{U} are made up of N functions $(u_1, \dots, u_j, \dots, u_N)$ characterizing self-oscillations of N oscillators, the elements of the diagonal matrix $\hat{\Delta}(\Delta_1, \dots, \Delta_N)$ are equal to the frequency mismatch of the oscillators relative to the natural frequency of the first oscillator with $\omega_1 = 1$, and d is the coefficient of coupling between the oscillators. The elements of matrix \hat{A} are equal to $a_{1,1} = a_{N,N} = -1$, $a_{j,j} = -2$, $a_{j+1,j} = a_{j,j+1} = 1$ ($j = 1, \dots, N-1$), while for all the rest $a_{i,j} = 0$. The parameter ϵ characterizes the smallness of the quantities standing after it, when the asymptotic methods are employed, and is omitted in final expressions.

Further consideration, except Sec. V, is carried out in a quasiharmonic approximation ($\epsilon \ll 1$) in its traditional interpretation. The fast ($\xi = \omega t$, $\omega = 1 + \epsilon \omega^{(1)} t + \dots$) and slow ($\eta = \epsilon t$) time dependences are introduced. Then, Eq. (2) is written, to an accuracy of the terms $\sim \epsilon^2$, in the form

$$\begin{aligned} (1 + 2\epsilon \omega^{(1)})u_{\xi\xi} + 2\epsilon u_{\xi\eta} + u - 2\epsilon(p\hat{I} - \hat{U}^2)u_{\xi} \\ = 2\epsilon(d\hat{A}u_{\xi} - \hat{\Delta}u). \end{aligned} \quad (3)$$

The solution is sought as an expansion $u^{(0)} + \epsilon u^{(1)} + 0(\epsilon^2)$ to an accuracy of the terms $0(\epsilon^2)$ to give a system

$$\begin{aligned} u_{\xi\xi}^{(0)} + u^{(0)} &= 0, \\ u_{\xi\xi}^{(1)} + u^{(1)} &= -2(p\hat{I} - \hat{U}^2)u_{\xi}^{(0)} - 2u_{\xi\eta}^{(0)} - 2\omega^{(1)}u_{\xi\xi}^{(0)} \\ &\quad + 2(d\hat{A}u_{\xi}^{(0)} - \hat{\Delta}u^{(0)}). \end{aligned} \quad (4)$$

From this it follows that

$$u^{(0)} = z(\eta)\exp(i\xi) + z^*(\eta)\exp(-i\xi), \quad (6)$$

where z is the vector column with components z_j . The complex amplitudes $z_j(\eta)$ are determined from the resolvability condition for the system (4), (5) that reduces in this case to requirement of the absence of resonance terms $\sim \exp(\pm i\xi)$ in the right-hand side of Eq. (5). If this requirement is fulfilled, we obtain the equation

$$\begin{aligned} \dot{z}_j &= i\Delta_j z_j + (p - z_j^2)z_j + d(z_{j+1} - 2z_j + z_{j-1}), \\ j &= 1, \dots, N, \\ z_0 &= z_1, \quad z_{N+1} = z_N. \end{aligned} \quad (7)$$

Equation (7) is a discrete analog of the Ginzburg-Landau equation. (Without loss of generality, we can suppose that

$\omega^{(1)}=0$ because the solutions in the approximation taken are invariant to $\omega^{(1)}$ if their final form is written in the initial variables.)

By passing to real amplitudes and phases, $z_j = \rho_j \exp(i\phi_j)$, we obtain a set of equations consisting of two groups that can be referred to as amplitude and phase ones, respectively:

$$\dot{\rho}_j = (p - \rho_j^2)\rho_j + d(\rho_{j+1}\cos\theta_{j+1} - 2\rho_j + \rho_{j-1}\cos\theta_{j-1}), \quad (8)$$

$$j = 1, \dots, N$$

$$\dot{\theta}_j = \bar{\Delta}_j + d \left[\frac{\rho_{j+2}}{\rho_{j+1}} \sin\theta_{j+1} - \left(\frac{\rho_j}{\rho_{j+1}} + \frac{\rho_{j+1}}{\rho_j} \right) \sin\theta_j + \frac{\rho_{j-1}}{\rho_j} \sin\theta_{j-1} \right], \quad j = 1, \dots, N-1 \quad (9)$$

$$\dot{\phi}_1 = \Delta_1 + d \frac{\rho_2}{\rho_1} \sin\theta_1. \quad (10)$$

Here, $\theta_j = \phi_{j+1} - \phi_j$ and $\bar{\Delta}_j = \Delta_{j+1} - \Delta_j$. We consider the following boundary conditions:

$$\rho_0 = \rho_1, \quad \rho_{N+1} = \rho_N, \quad \phi_0 = \phi_1, \quad \phi_{N+1} = \phi_N. \quad (11)$$

Below in this section we set $\bar{\Delta}_j = \Delta$ for all j .

We take as the synchronization conditions the coincidence of averaged partial frequencies Ω_j estimated as the $2\pi n_j(T)/T$ ratio, where $n_j(T)$ is the number of typical features of the time series (e.g., the maxima exceeding certain values) in the time interval T . A qualitative picture of the spatio-temporal structure of oscillations was obtained by plotting shadowgraphs of $z_j(t)$ on the (j,t) plane. Arrays of 100 elements at $p=0.5$ were investigated in all experiments.

B. Global synchronization in an assembly.

Stationary phase distributions.

Synchronization band

A stable equilibrium state in the system of equations (8) and (9) corresponds to the regime of global synchronization in the array. For the synchronous regime ($\dot{\rho}_j=0$, $\dot{\theta}_j=0$), amplitude equations in a zero approximation give the same oscillation amplitudes for all elements of the array. Then, with allowance made for the condition $\bar{\Delta}_j = \Delta$, the system of equations for the stationary phase differences $\bar{\theta}_j$ is rewritten in the form

$$\Delta + d(\sin\bar{\theta}_2 - 2\sin\bar{\theta}_1) = 0, \quad (12)$$

$$\Delta + d(\sin\bar{\theta}_{j-1} - 2\sin\bar{\theta}_j + \sin\bar{\theta}_{j+1}) = 0, \quad j = 2, \dots, N-2 \quad (13)$$

$$\Delta + d(\sin\bar{\theta}_{N-2} - 2\sin\bar{\theta}_{N-1}) = 0. \quad (14)$$

As follows from [16], the distribution of $\bar{\theta}_j$ is equal to

$$\sin\bar{\theta}_j = \frac{\Delta}{2d} (Nj - j^2). \quad (15)$$

It follows from Eq. (15) that the system (13) has 2^{N-1} equilibrium states (see, e.g., [18,21]) and only one of them (for $-\pi/2 < \bar{\theta}_j < \pi/2$) is stable. As the frequency mismatch Δ is increased, the condition of synchronization for all elements:

$$\left| \frac{\Delta}{2d} (Nj - j^2) \right| < 1, \quad (16)$$

that coincides with the condition of the existence of equilibrium states [21], is violated first for $j=N/2$ at even N , i.e., for the middle element of the array. Thus the condition of global synchronization in the array (or the respective synchronization band) is given by the inequality

$$\left| \frac{\Delta N^2}{8d} \right| < 1. \quad (17)$$

The correction to the frequency of synchronized oscillations, $\Delta\omega_c$, may be determined from the equation for phase ϕ_1 :

$$\dot{\phi}_1 = d \sin\bar{\theta}_1 + \Delta, \quad (18)$$

so that

$$\Delta\omega_c = \Delta(N-1)/2. \quad (19)$$

For $\Delta = 8d/N^2$, we have the following stationary values: $\bar{\theta}_{N/2} = \pi/2$. In this case, the stable and unstable equilibrium states merge and a rotatory (with infinite growth of phase differences $\theta_{N/2}$) periodic motion is born in the phase space of the system of equations for phase difference. All the elements of the array are coupled. Consequently, as the phase difference between the middle element and its neighbor increases, the stationary regime of global synchronization changes to the regime of oscillations $\theta_j(t)$ near a certain constant value of θ_j , with the oscillation amplitude depending on j in all elements of the array. The closer the elements are to the ends of the array, the smaller the amplitude of oscillations is. In the case of a long array, the current values of θ_j are nearly constant (or constant) for the edge elements, i.e., the regime of synchronization occurs. Thus the array is divided into two clusters of equal sizes ($N/2$) that consist of mutually synchronized elements at different average frequencies.

C. Regimes of cluster synchronization

Two principal regimes are realized, as Δ/d is increased, depending on the values of the parameters. The first of them is the regime of multifrequency generation, when most elements of the array (except, perhaps, the edge ones) generate different frequencies as in Figs. 1(a) and 1(b). The second one is the regime of cluster synchronization, when all the oscillators are divided into several groups inside which all the elements oscillate at the same average frequency [Fig. 1(b), Fig. 2]. The values of frequency for each cluster (except the edge ones) are close to those obtained by averaging natural frequencies over all the elements forming the cluster. In the considered case of linear dependence of frequency on

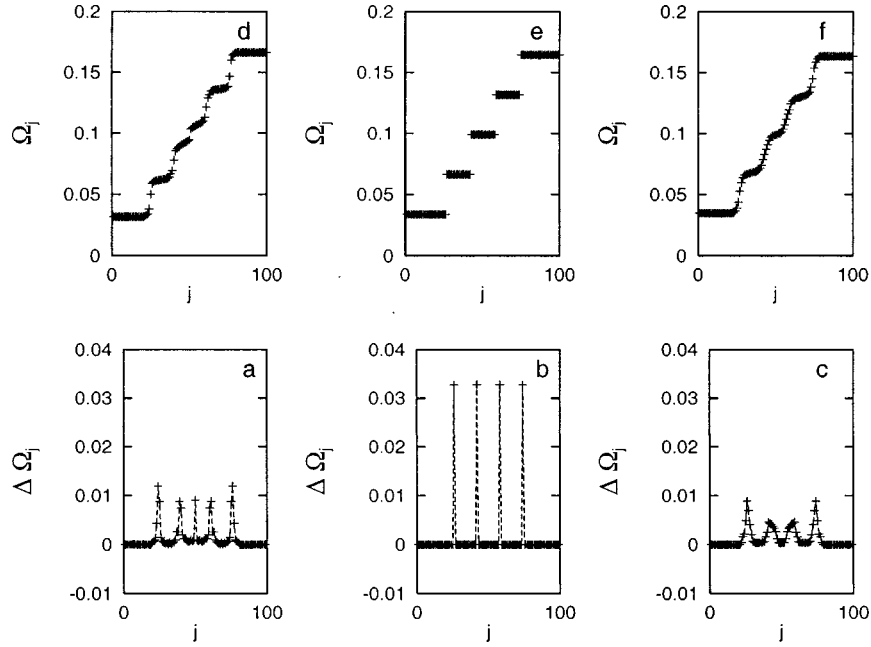


FIG. 1. Averaged frequencies Ω_j and their difference $\Delta\Omega_j = \Omega_{j+1} - \Omega_j$ for perfect (b), (e) ($d=1.2$) and intermediate (a), (d) ($d=1.0$), (c), (f) ($d=1.45$) cluster structures for $\Delta = 2 \times 10^{-3}$.

j in Fig. 2, this corresponds to the intersection of the lines $\Omega = \Omega_j = \phi_j$ and $\Omega = j\Delta$ exactly in the middle of the cluster. These cluster structures are periodic in time. The frequency differences between the clusters in such structures coincide and are equal to the lowest cluster frequency [in terms of the amplitude equations (7)]:

$$\Omega_n = \Delta(N-1)/(n+1). \quad (20)$$

The size of the clusters N_n for small Δ may be approximated, to an accuracy of ± 1 element, by the relations for the middle clusters:

$$N_n = \frac{N-1}{n+1}, \quad (21)$$

and for the edge clusters:

$$N_n = \frac{3}{2} \frac{N-1}{n+1}. \quad (22)$$

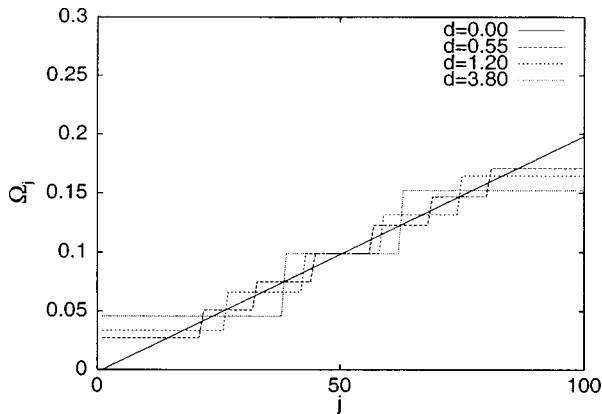


FIG. 2. Averaged frequencies Ω_j for different values of coupling coefficients d in the case $\Delta = 2 \times 10^{-3}$.

Here, N ($=100$) is the number of elements and n ($=2, \dots$) is the number of clusters. The sizes of middle clusters N_n at the instant they break are plotted in Fig. 3. The scaling by parameters Δ and d is similar to the one that specifies, in the constant amplitude approximation ($|z_j| = |z_0|$), the limiting size of the array with free ends in which the global synchronization (17) may occur:

$$N_n \sim \left(\frac{8d}{\Delta} \right)^{1/2}. \quad (23)$$

The spatiotemporal behavior of cluster structures is illustrated in Fig. 4, where the darker regions mark the higher values of intensities of $|z_j|^2$ [Fig. 4(a)] and real parts $\text{Re } z_j$ [Fig. 4(b)] of complex amplitudes of oscillations. Oscillograms of intensities for the middle elements of the array are shown in Fig. 5. Detailed comparison of the data given in these figures as well as in Fig. 1 leads to a conclusion that perfect cluster structures may be formed (for $d=0.8, 1.2, 1.8$ in Figs. 1 and 4).

The intensity of $|z_j|^2$ decays periodically almost to zero at the cluster boundaries [Fig. 5(b)]. With increasing distance from the boundary of the clusters, the magnitude of intensity drops decreases so that the change of the real part of complex amplitudes z_j in the (j, t) plane shown in Fig. 4(b) represents correctly the phase of z_j . The formation of a defect in the spatiotemporal pattern of the phase (or $\text{Re } z_j$), that is visualized as the singularity of the intensity field of $|z_j|^2$, corresponds to the transition between the clusters.

Since the number of the defects, n_D , formed in one period of a perfect cluster structure is a unity less than the number of clusters n and their repetition rate is $T = 2\pi\Omega_n^{-1}$, the number of the defects per unit time is equal to

$$\rho_D = \frac{n_D}{T} = \frac{\Delta(N-1)}{2\pi} \frac{n-1}{n+1}. \quad (24)$$

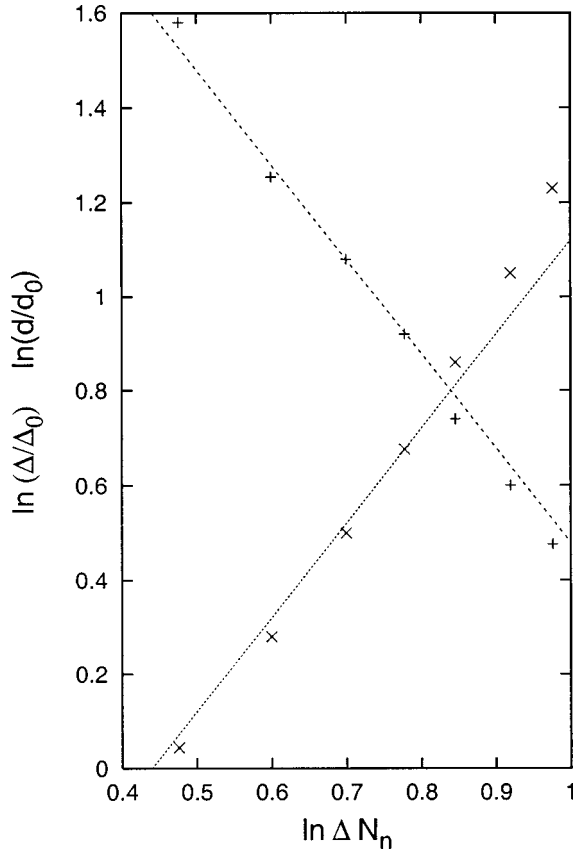


FIG. 3. Critical values of frequency gradient (\times) in the range $\Delta \approx (0.5-17) \times 10^{-3}$ for $d=1$ and coupling coefficient ($+$) in the range $d \approx 0.3-3.8$ for $\Delta = 2 \times 10^{-3}$, at which the n -cluster structure breaks prior to transition from the n th to the $(n+1)$ th cluster depending on the size of middle clusters N_n . The scale is logarithmic to an accuracy of arbitrarily chosen origin; the straight lines correspond to the dependence (21).

Estimates by these formulas agree well with the data obtained directly from numerical solutions. In particular, the number of the defects is equal to 44, 40, and 39 for the case shown in Fig. 4(a) at $d=0.8, 1.2$, and 1.8 , and to 45, 42, and 38, respectively, when calculated by the formula (24). Note that, when the transitions between the structures with n and $n+1$ clusters are caused by changes of coupling coefficient d , the average defect density changes only slightly at $n \geq 4$. At the same time, their relative position in the (j, t) plane alters significantly. For example, in Fig. 4(a) it changes from completely ordered at $d=1.2$ to irregular at $d=1.45$, and then again to a regular one but now with a different symmetry at $d=1.8$. The time series undergo the corresponding changes too (see Fig. 5).

We will mention here some consequences of the scalings (23) and (24) for two limiting transitions to infinitely long arrays $N \rightarrow \infty$ at a constant interval of oscillator frequencies $\Delta \omega_\Sigma = \Delta N = \text{const}$. In the first of these two transitions (thermodynamic), the coupling coefficient d remains constant $d_N = D = \text{const}$. In the second one (“continuous”), the coupling coefficient $d_N = DN^2$, so that the corresponding second-order difference in Eqs. (2) and (7) tends to the second derivative with respect to the spatial coordinate. As follows from Eq. (23), the maximal size of the clusters in the thermodynamic limit changes as

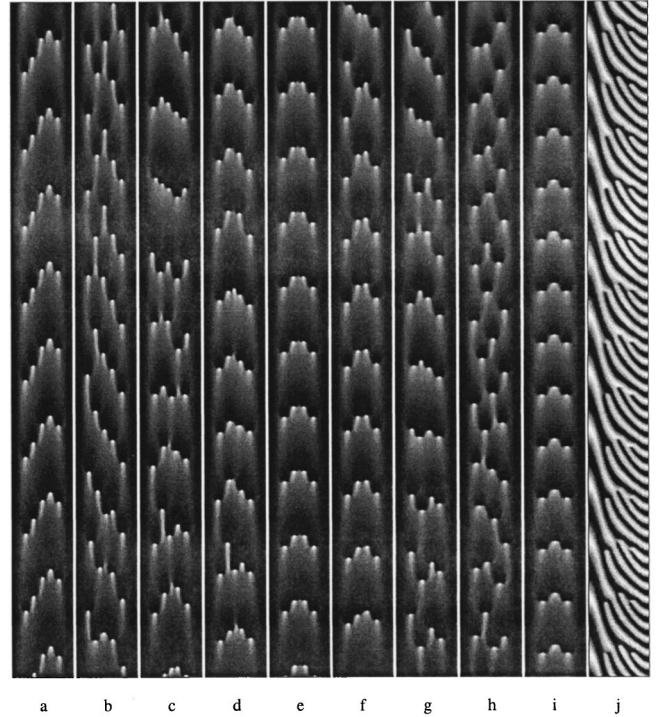


FIG. 4. Space-time diagrams: (a)–(i) intensities of $|z_j|^2$ and (j) real parts $\text{Re } z_j$ for $\Delta = 0.002$ and different values of coupling coefficients: 0.8 (a); 0.9 (b); 1.0 (c); 1.1 (d); 1.2 (e); 1.3 (f); 1.45 (g); 1.6 (h); 1.8 (i), (j). The spatial coordinate $j = 1, \dots, 100$ is plotted on the abscissa axis, and time $t \in [0, 2000]$ on the ordinate axis.

$$N_n \sim \left(\frac{8DN}{\Delta \omega_\Sigma} \right)^{1/2}.$$

Consequently, their relative size \bar{N}_n/N and the interval of variations of natural frequencies along the cluster length, $\bar{N}_n(\Delta \omega_\Sigma)/N$, tend to zero as the number of elements is increased. At the same time, the quantities N_n/N and $\bar{N}_n(\Delta \omega_\Sigma)/N$ change approximately as $[(8ND)/\Delta \omega_\Sigma]^{1/2}$ in the “continuous” limit. As a result, the regime of global synchronization $N_1 = N$ will inevitably be established as $N \rightarrow \infty$. The mean density of defects in the (j, t) plane, as is seen from Eq. (24), will remain constant in either case, of course, if we speak about the range of the parameters in which the number of clusters is much greater than unity.

Both the picture of synchronization presented above and its description in a rather general form on the basis of numerical solutions are possible due to high degree of symmetry and homogeneity of the problem in a quasiharmonic approximation at small frequency gradients and coupling coefficients. Actually, the meaningful quantity in this approximation is not the frequency itself but the frequency difference Δ_j . Consequently, the system may be regarded to be a homogeneous one at $\Delta_j = \Delta = \text{const}$ if the edge effects are neglected. The picture is becoming more complicated, as Δ and d are increased. This makes the effects of multistability and the changes of the amplitudes of oscillations along the array essential.

D. Multistability

Investigations into processes of cluster structure formation revealed multistability, the most vivid manifestation of

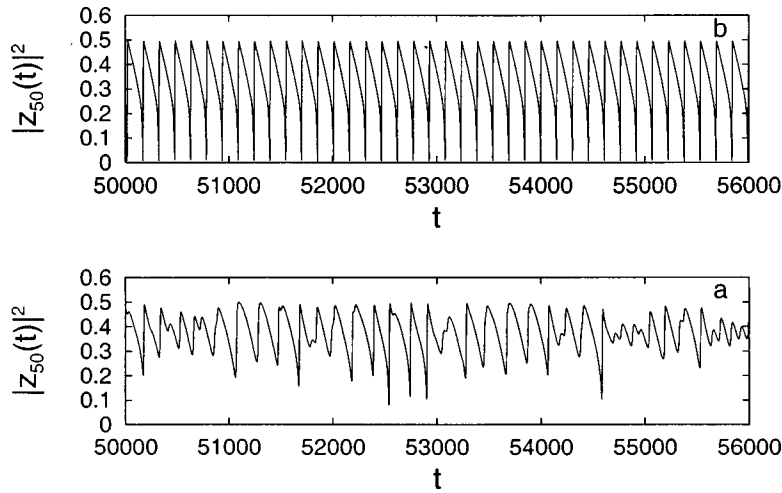


FIG. 5. Intensity oscillograms for the middle elements of the array for $\Delta=0.002$: (a) $d=1.45$ and (b) $d=1.8$.

which is formation of the structures containing a different number of clusters depending on initial conditions. The existence domains of the structures having a definite number of clusters obtained in numerical experiment with adaptation of the initial conditions to small variations of the parameters are shown in Fig. 6. The adaptation procedure was as follows: The mismatch Δ was varied successively by $+5 \times 10^{-4}$ or by -5×10^{-4} . The values from the steady-state solution obtained in the previous variant were taken as the initial conditions for $z_i(t)$. Although the procedure described does not guarantee that all possible regimes will be found, it enables us to reveal qualitatively different transitions in the domain, where the states possessing a different number of clusters coexist, i.e., in the region of multistability and in the region of parameters where it is absent. In the first case, as Δ increases by less than 5×10^{-4} , a ‘‘hard’’ transition without intermediate structures occurs from the state with four clusters to the state with five clusters. In the second case, a ‘‘soft’’ transition occurs at a much greater interval of variations $\Delta \approx 2.2 \times 10^{-3}$, with a smooth transition of intermediate structures one into another (Fig. 7).

Note that a nonmonotonic dependence of the number of clusters on the magnitude of frequency mismatch (Fig. 8) is observed in the region of multistability when solutions under

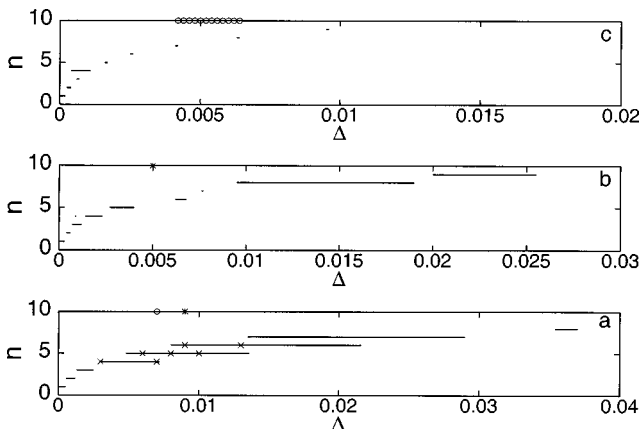


FIG. 6. The ranges of frequency gradients at which structures with n perfect clusters of the type shown in Fig. 1(b) are given for coupling coefficients $d=1,2,5$.

the same initial conditions are sought. Namely, $x_j(0) \equiv \text{Re}[z_j(0)] = -0.01$ for even j , $x_j(0) = 0.01$ for odd j , and $y_j(0) \equiv \text{Im}[z_j(0)] = 0.01$ for all j . This is evidently due to an intricate structure of the basins of the corresponding attractors in phase space, the deformation of which leads to the alternating initial conditions in each of them. This lays the basis (see Sec. IV A) for one of the methods of governing the processes of formation of the structures of mutually synchronized elements.

The sophisticated structure of the phase portrait of the system considered does not exclude that multistable regimes of other types, when the structure of the clusters rather than their number is changed, may also be observed. For verification of this hypothesis we conducted a series of experiments in which the amplitude and phase distributions formed earlier in the clusters but now with a different number of elements were taken as initial conditions. Usually, the number of elements in the cluster was changed by $N_n = \pm 1, 2$. It was found that the same cluster structure was always established in the region of the parameters of interest with such variations of initial conditions.

III. ‘‘OSCILLATOR DEATH’’

A distinguishing feature of cluster synchronization with a still further increase of coupling d and mismatch Δ is the

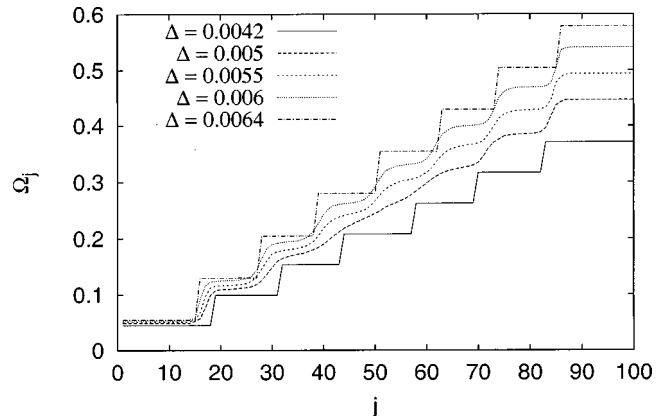


FIG. 7. Averaged frequencies Ω_j in the soft transitions from n to $n+1$ clusters. The corresponding regions of parameters are indicated in Fig. 6 by \circ .

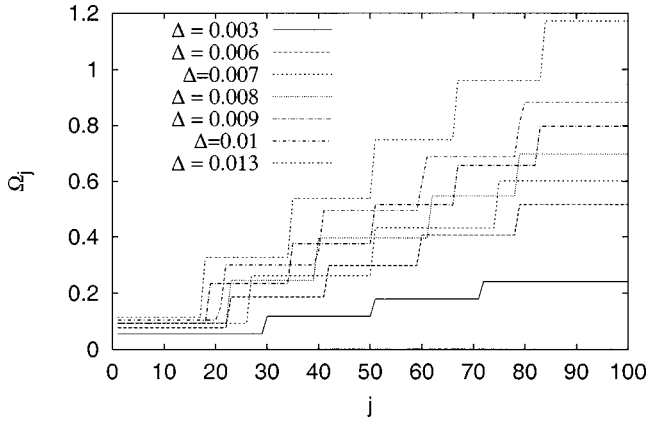


FIG. 8. Nonmonotonic sequence of the number of clusters (4,5,4,5,6,5,6 upwards) at monotonic variation of frequency gradient Δ and identical initial conditions ($d=5$). The corresponding values of the parameters are marked in Fig. 6 by \times .

formation of clusters separated by a region of unexcited oscillators [17,18]. The formation of such regions may be interpreted as manifestation of the effect of oscillator death [6–9,19]. Recall (see, e.g., [19]) a bifurcation diagram for two coupled oscillators the qualitative plot of which is given in Fig. 9. It is similar to the diagram for an assembly of oscillators coupled all to all, with the frequencies distributed uniformly in a narrow interval $\Delta\omega_\Sigma$.

Depending on the qualitative properties of the solutions, one can distinguish in the diagram three main regions: (1) the region of oscillator death in which a trivial solution is stable (we remind the reader that we consider the case when the self-excitation condition $p > 0$ is fulfilled for uncoupled oscillators); (2) the synchronization region $\dot{\phi}_1 = \dot{\phi}_2$; and (3) the region of nonsynchronized oscillations $\lim_T T^{-1}(\phi_1 - \phi_2) \neq 0$. The transition between regions 2 and 3 has a complicated structure, with both regularly and chaotically modulated oscillations possible in a general case. The transitions between regions 1 and 2 or 1 and 3 are much simpler and are determined from analysis of the stability of trivial solution. For two oscillators ($N=2$), the eigenvalues for small perturbations are equal to

$$\lambda_{1,2} = p - d \pm \sqrt{d^2 - (\Delta/2)^2},$$

where $\Delta = \omega_2 - \omega_1$ is the frequency difference of the oscillators. There occurs the transition to a double-frequency regime if $d=p$, $\Delta > 2d$, and to a single-frequency regime if $d = (\Delta^2/4 - p^2)/2p$, $\Delta < 2d$ (Fig. 9).

All the solutions mentioned above are observed in an assembly of coupled oscillators. By virtue of collective effects, they may be realized either globally (in all elements) or locally (in clusters of neighboring elements).

For better understanding of the transitions in long arrays, the following interpretation of oscillator death may be useful. Consider a linearized equation for one of the oscillators:

$$\dot{z}_2 = i\Delta z_2 + pz_2 + d(z_1 - z_2).$$

Here, the term containing the oscillation amplitude of the first oscillator, on breaking of synchronization, may be regarded as a nonresonant external force, and the second term

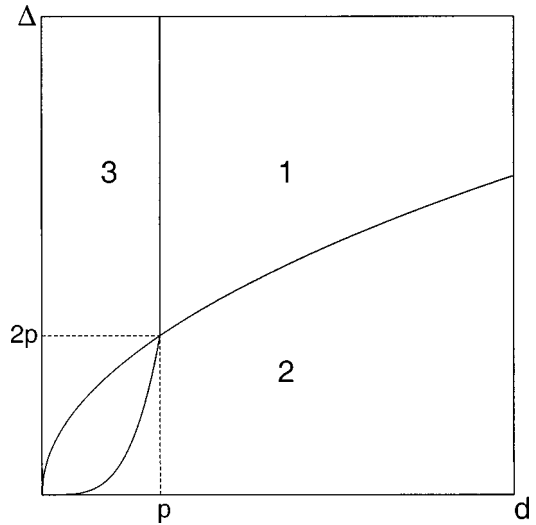


FIG. 9. Bifurcation diagram of the system of two coupled oscillators: (1) region of oscillator death where a trivial solution is stable; (2) region of synchronization; (3) region of nonsynchronized oscillations.

that depends on the magnitude of coupling $-dz_2$ exerts the same effect as additional losses. If the losses do not exceed the amplification ($d < p$), a double-frequency regime is possible. For $d > p$, there remain only forced oscillations with the amplitude $\rho_2 = d/|i\Delta + p - d|$ decreasing as the mismatch Δ is increased.

An analogous mechanism of oscillator death is observed in an array. An essential aspect in this case is that, with the increase of mismatch Δ , the synchronization conditions are violated locally and not all at once throughout the array, namely, in the neighborhood of the weakest element of the array, i.e., in the middle of the array at the site where the regime of global synchronization breaks earliest (see Sec. II B). In this case, for sufficiently great mismatches, i.e., when the influence of the neighbors is no longer a resonant one, the coupling acts as effective damping, and for $2d > p$ the corresponding element becomes unexcited. As Δ is increased, the region of oscillator death is expanding so fast that there remain only two clusters that are not fractioned due to local desynchronization any longer because the increase of the parameter Δ/d , that usually leads to breaking of synchronization, is compensated by the decrease of the size of the clusters (see [6,21]). This is illustrated in Fig. 10, where two clusters of synchronized elements at the edges of the array are separated by an area of unexcited oscillations.

IV. THE EFFECT OF NONUNIFORMITY OF FREQUENCY MISMATCH GRADIENT ON FORMATION OF SYNCHRONIZED CLUSTERS

A. Sensitivity of the structures to regular nonuniformities

We can distinguish at least two mechanisms controlling the spatial structure of the system of interest, when additional inhomogeneities of the frequency gradient Δ_j periodic along the array are introduced. One of them is associated with transformation of an attractor (or attractors). The other one is attributed to changes only of attraction basins (see, e.g., [4,5,22]). It can be expected that the second mechanism

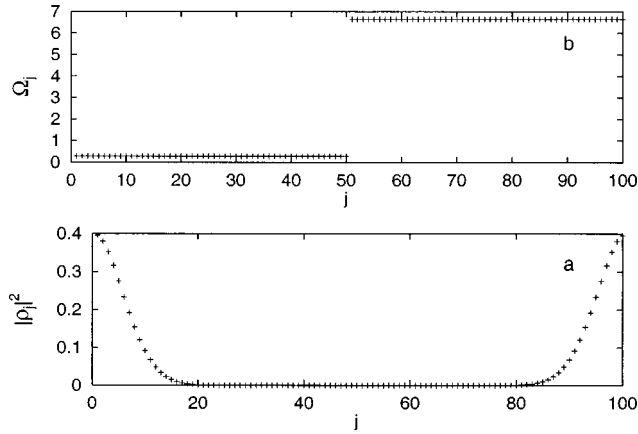


FIG. 10. (a) Squared mean amplitudes $|\rho_j|^2$ and (b) averaged frequencies Ω_j in the case of oscillator death in the array for $d=5$, $\Delta=0.06$. There are two clusters consisting of 20 mutually synchronized elements at the ends of the array.

is readily realized in the above-mentioned case of nontrivial dependence of the number of clusters on the magnitude of frequency mismatch gradient. Indeed, for the parameter values and initial conditions like in Fig. 6 (marked with an asterisk for $d=5$), a relatively small, periodic along j correction to the natural frequencies:

$$\omega_j = \Delta(j-1) + \alpha \sin\left(\frac{2\pi n^*(j-1)}{N}\right) \quad (25)$$

leads to the change of the number of clusters formed [22]. Particularly, for $\Delta=0.009$ and $n^*=5$, the number of clusters is $n=6$ if $\alpha=0$, and $n=5$ if $\alpha=0.0001$. By introducing a perturbation with a much larger amplitude $\alpha \geq 0.002$, one can influence not only the process of cluster formation in the regime of transition but also the structures that have already been formed. For example, the transition from six to five clusters occurs for $d=5.0$; $\alpha=0.002$; $\Delta=0.009$ [see Fig. 6(a)]. This case corresponds to the first mechanism of forcing, namely, destruction of one of the multistable states, in this case, the structure of six clusters. Another possible manifestation of this mechanism is formation of synchronization clusters from a nonsynchronized state, when the transition from a chaotic state in space and time to a state with five clusters takes place (Fig. 11).

Note that the expression (25) does not give a clear picture of the relationship between the magnitudes of uniform and nonuniform components of frequency mismatch. Only comparison either of their gradients or of their changes over the modulation period along the array is physically meaningful. By comparing these quantities one can see that the perturbation is determined by the parameter $(\alpha/\Delta)(2\pi n/N)$ that did not exceed $\frac{1}{3}$ in all the cases considered.

B. The effect of random dispersion of natural frequencies on cluster synchronization

We restrict our consideration to one aspect of the effect exerted by spatially irregular parameter variations on the formation of synchronized structures. Namely, we investigate the dependence of spatial structures on the magnitude of random distribution of mismatch relative to some mean at a

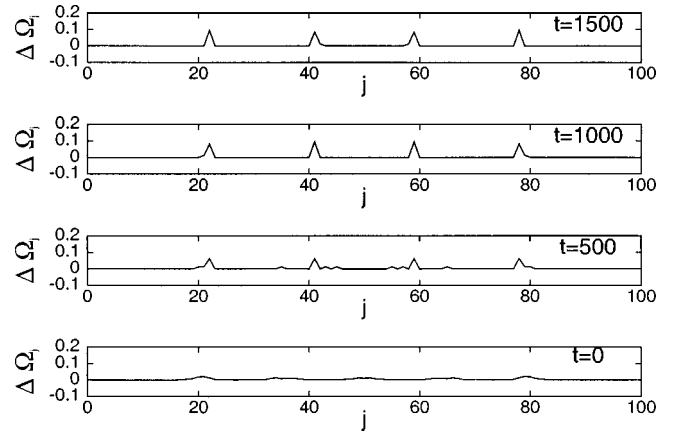


FIG. 11. Restructuring under the action of periodic inhomogeneity: $d=2$, $\Delta=0.005$, $\alpha=0.005$ [see Fig. 6(b)]. The frequencies were determined by averaging over time $\Delta t=500$ prior to subsequent record of Ω_j distribution.

constant complete range of frequency variations according to the expression (1). The critical values of d averaged over 20 samples of random numbers, at which the transition between cluster structures occurs, are presented in Fig. 12. The regime of global synchronization is established at much smaller values of coupling for random frequency distribution than for linear frequency distribution. This effect was actually observed for each space series of random frequency distribution.

V. SYNCHRONIZATION IN AN ARRAY OF VAN DER POL OSCILLATORS

We have already mentioned that the picture of synchronization described above and simple scalings at linear variation of natural frequencies along the array are due to high degree of symmetry and homogeneity of the problem. This is true, on the other hand, if the array is sufficiently long so that the edge effects do not introduce significant distortions into clusters. On the other hand, the quasiharmonic approximation

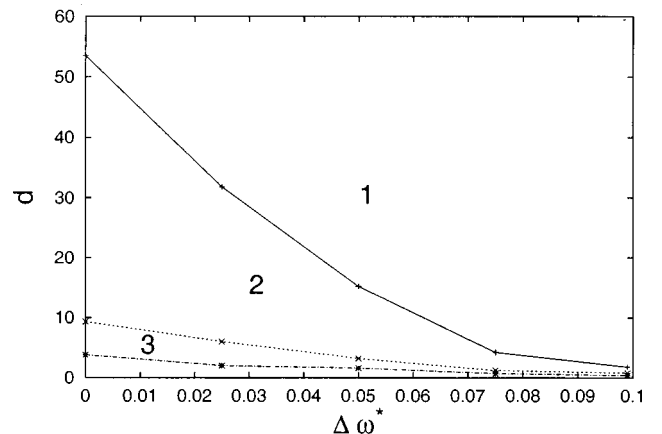


FIG. 12. Average critical values of d at which the transition between different cluster structures occurs for $\Delta=0.002$. Region 1 corresponds to the regime of global synchronization. Two and three clusters of mutually synchronized elements exist in regions 2 and 3, respectively. The averaging was made over 20 sample random natural frequencies.

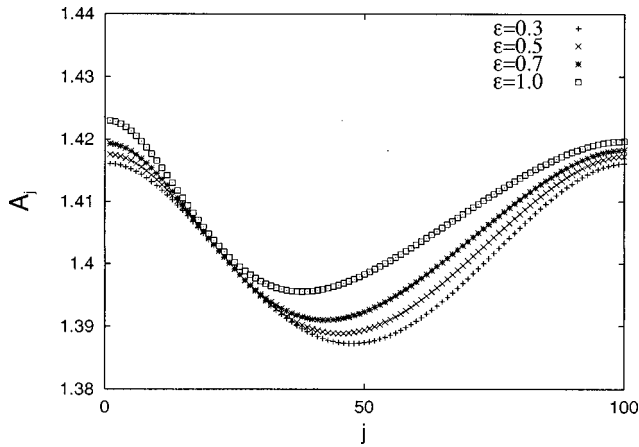


FIG. 13. Mean amplitudes $A_j = \sqrt{u_j^2 + \dot{u}_j^2}$ for different values of ϵ in the case $d=5$, $\Delta=0.00025$.

should be valid, $\epsilon \ll 1$, when not natural frequencies but their gradient is the essential parameter. The situation changes cardinally with the increase of ϵ because nonlinear distortions of the shape of oscillations become pronounced. Since these distortions are greater in the low-frequency region than in the high-frequency one, the symmetry of the problem is violated. In particular, the amplitude distribution becomes essentially nonsymmetric (Fig. 13) even at stable synchronization for small Δ , when the amplitude modulation is several percent. As a result, the distribution of stationary phase differences of the neighbors that matches the amplitude distribution is no longer symmetric. Consequently, the regime of global synchronization is broken in the elements close to the beginning of the array rather than in the middle elements (Fig. 14). In spite of the strong dependence of the shape of oscillations on nonlinearity ϵ , one can observe in the interval of its intermediate values $\epsilon \approx 1$ an almost linear relationship between ϵ and the critical value of mismatch, Δ^* , starting from which the regime of global synchronization breaks. The linear relationship exists also between ϵ and the squared size

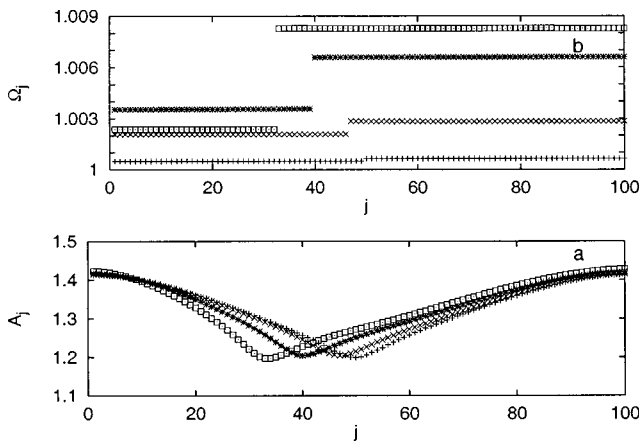


FIG. 14. (a) Mean amplitudes $A_j = \sqrt{u_j^2 + \dot{u}_j^2}$ and (b) averaged frequencies Ω_j at different values of ϵ and Δ for $d=5$. The curves are marked by + for $\epsilon=0.02$ and $\Delta=0.0006$; by \times for $\epsilon=0.1$ and $\Delta=0.0006$; by $*$ for $\epsilon=0.3$ and $\Delta=0.00065$; and by \square for $\epsilon=0.5$ and $\Delta=0.0007$. The values of Δ are slightly larger than the critical values Δ_{cr} at which the regime of global synchronization is disturbed.

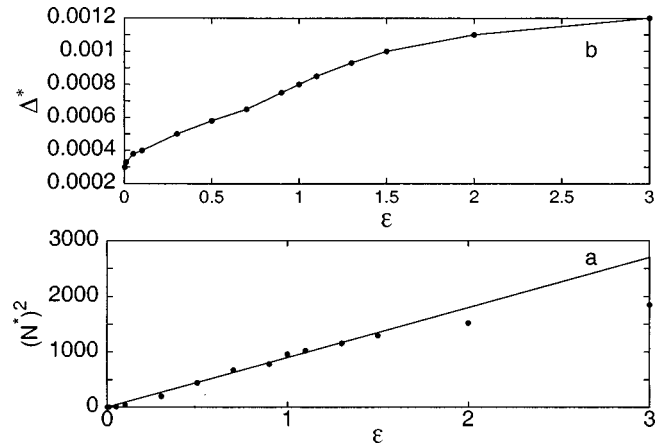


FIG. 15. (a) The dependence on ϵ of the squared quantity $N^* = 50 - N_c$, where N_c is the length of the smaller of the two synchronization clusters that are formed after breaking of the regime of global synchronization; (b) the dependence on ϵ of the critical value of mismatch Δ^* starting from which the regime of global synchronization is not realized: $N=100$, $d=5$.

of the smallest of the two clusters formed as the global synchronization breaks. Examples of such relationships are given in Fig. 15.

VI. CONCLUSION

The collective behavior of an array of diffusively coupled Van der Pol oscillators at weak and relatively strong nonlinearity has been investigated employing asymptotic and numerical methods. Typical features of the onset and existence of the regimes of global (all-to-all) and cluster (partial) synchronization have been explored. Two scenarios, “soft” and “hard,” of the transitions between the structures consisting of a different number of synchronization clusters have been revealed. In the first case, gradual tuning of spatial distribution of averaged frequencies is observed. In the second case, the transition from the structure of n synchronized clusters to the structure of $n+1$ clusters occurs in a stepwise fashion as a consequence of multistability.

The effect of different types of natural frequency distributions on synchronization in a constant range of frequency variations is investigated. It is revealed that the characteristics of the synchronization are improved when an irregular distribution of natural frequencies is used.

Note that many of the effects observed in the arrays of coupled periodic oscillators were also revealed in analysis of the regimes of chaotic phase synchronization in an array of coupled Rössler oscillators [23].

The formation of synchronized clusters was observed in some systems in which the distribution of natural frequencies is almost linear. For example, the measured electrical activity along the (intact) mammalian intestine displays frequency plateaus [24]. The stepwise dependence of frequency on the axial coordinate was also observed in the flow around a cone-shaped cylinder [25]. It was established that in both cases (see the papers [16] and [24], respectively) these phenomena resemble the effects of cluster synchronization in the model of coupled oscillators. At the same time, it was revealed that the shape of the clusters in each particular case

should be described taking into consideration subtle details of frequency distribution and features of interaction. As follows from the above consideration, one of the reasons for such a sensitivity is a high degree of symmetry and uniformity of the problem in the presence of a uniform frequency gradient. Even a small perturbation, that breaks the symmetry, may lead to substantial changes of cluster structure in such a situation. An illustrative example are the frequency distributions given in Fig. 15 for different values of nonlin-

earity parameter ϵ . There are no such nonsymmetric clusters in the frame of the Ginzburg-Landau equations.

ACKNOWLEDGMENTS

This research was done under the financial support of the Russian Foundation for Basic Research (Project No. 96-02-18041), the "Leading Scientific Schools" Program (Project No. 96-15-96593), and the National Science Foundation (G.V.O.).

-
- [1] L. Sh. Tsimring, Phys. Rev. E **48**, 3446 (1993).
 [2] L. N. Korzinov and M. I. Rabinovich, Izv. Vyssh. Uchebn. Zaved. Prikladnaya Nelinejnaya Dinamika **2**, 59 (1994) (in Russian).
 [3] M. Bazhenov, M. Rabinovich, and L. Rubchinsky, J. Stat. Phys. **83**, 1165 (1996).
 [4] Y. Braiman, J. F. Lindner, and W. L. Ditto, Nature (London) **378**, 465 (1995).
 [5] Y. Braiman, W. L. Ditto, K. Wiesenfeld, and M. L. Spano, Phys. Lett. A **206**, 54 (1995).
 [6] Y. Yamaguchi and H. Shimizu, Physica D **11**, 212 (1984).
 [7] K. Bar-Eli, Physica D **14**, 242 (1985).
 [8] G. B. Ermentrout, in *Nonlinear Oscillations in Biology and Chemistry*, edited by H. Othmer, Lecture Notes in Biomathematics Vol. 66 (Springer, Berlin, 1986).
 [9] G. B. Ermentrout and W. C. Troy, SIAM (Soc. Ind. Appl. Math.) J. Appl. Math. **39**, 623 (1986).
 [10] N. E. Diamant, P. K. Rose, and E. J. Davidson, Am. J. Physiol. **219**, 1684 (1970).
 [11] B. R. Noak, F. Ohle, and H. Eckelman, J. Fluid Mech. **227**, 293 (1991).
 [12] S. K. Sarna, E. E. Daniel, and Y. I. Kinoma, Am. J. Physiol. **221**, 166 (1971).
 [13] D. Robertson-Dunn and D. A. Linkens, Med. Biol. Eng. Comput. **12**, 750 (1974).
 [14] B. H. Brown, H. L. Duthie, A. R. Horn, and R. H. Smallwood, Am. J. Physiol. **229**, 384 (1975).
 [15] R. J. Patton and D. A. Linkens, Med. Biol. Eng. Comput. **16**, 195 (1978).
 [16] G. B. Ermentrout and N. Koppel, SIAM (Soc. Ind. Appl. Math.) J. Math. Anal. **15**, 215 (1984).
 [17] S. D. Drendel, N. P. Hors, and V. A. Vasiliev, *Dynamics of Cell Populations* (Nizhny Novgorod University Press, Nizhny Novgorod, 1984), p. 108 (in Russian).
 [18] V. A. Vasiliev, Yu. M. Romanovsky, and V. G. Yakhno, *Autowave Processes* (Nauka, Moscow, 1987) (in Russian).
 [19] G. B. Ermentrout, Physica D **41**, 219 (1990).
 [20] D. G. Aronson, G. B. Ermentrout, and N. Koppel, Physica D **41**, 403 (1990).
 [21] V. S. Afraimovich, V. I. Nekorkin, G. V. Osipov, and V. D. Shalfeev, *Synchronization, Structures and Chaos in Nonlinear Synchronization Networks* (World Scientific, Singapore, 1995).
 [22] G. V. Osipov and M. M. Sushchik, IEEE Trans. Circuits Sys. I: Fundam. Theory Appl. **44**, 1006 (1997).
 [23] G. V. Osipov, A. S. Pikovsky, M. G. Rosenblum, and J. Kurths, Phys. Rev. E **55**, 2353 (1997).
 [24] N. Diamant and A. Bortoff, Am. J. Physiol. **216**, 301 (1969).
 [25] B. R. Noak, F. Ohle, and H. Eckelmann, J. Fluid Mech. **227**, 293 (1991).